Supporting Information for:

$RbMgCO_3F$: A Beryllium-Free New Deep-Ultraviolet Nonlinear Optical Material

T. Thao Tran[1], Jiangang He,[2] James M. Rondinelli[2,] and P. Shiv Halasyamani[1,*]*

[1]Department of Chemistry, University of Houston, 112 Fleming Building, Houston, TX 77204-5003, USA

[2]Department of Materials Science and Engineering, Northwestern University, 2220 Campus Drive, Evanston, IL 60208-3108, USA

CORRESPONDING AUTHOR EMAIL ADDRESS: psh@uh.edu, jrondinelli@northwestern.edu.

Table of contents

Experimental section

Synthesis

Polycrystalline $RbMgCO_3F$ was synthesized through solid-state reactions. For $RbMgCO_3F$, stoichiometric amounts of RbF (4.0 mmol, 99.9% Alrich) and $MgCO_3$ (4.0 mmol) were thoroughly ground and pressed into a pellet. The pellet was placed in alumina boat that was heated to 330°C, held for 5 days, with intermittent re-grindings and then cooled to room temperature at a programmed rate of 180°C h^{-1}.

Crystals of $RbMgCO_3F$ were grown from hydrothermal techniques. the reaction mixtures of polycrystalline $RbMgCO_3F$ (3.0 mmol), RbF (0.3 mmol) and H_2O (2.0 mL) were placed separately in 23 mL Teflon-lined stainless steel autoclaves. The autoclaves were closed, gradually heated up to 200°C, held for 7 days, and then slowly cooled to room temperature at a programmed rate of 6°C h^{-1}. The solid products were isolated from the mother liquor by vacuum filtration and washed with ethanol. Colorless bock-shaped crystals, subsequently determined to be $RbMgCO_3F$, were obtained in approximately 70% yields based on starting polycrystalline $RbMgCO_3F$.

Structure determination: Single-crystal X-ray diffraction

A colorless block-shaped crystal (0.10 × 0.08 × 0.07 mm) was selected for single-crystal diffraction analysis. Data were collected on a Bruker DUO platform diffractometer equipped with a 4K CCD APEX II detector using graphite-monochromated Mo-Kα radiation at room temperature. A hemisphere of data (3061 frames at 6 cm detector distance) was collected using a narrow-frame algorithm with scan widths of 0.30° in omega and an exposure time of 60 seconds per frame. The data were integrated using the SAINT-V7.23A program,[1] with the intensities

corrected for Lorentz factor, polarization, air absorption, and absorption attributable to the variation in the path length through the detector faceplate. SADABS absorption corrections were applied based on the entire data.[1] Redundant reflections were averaged. Final cell constants for $RbMgCO_3F$ were refined using 4664 reflections having $I > 10\sigma(I)$.

The positions of the Rb and Mg atoms were determined by Direct methods using SHELXS-97,[2] and the remaining atoms were located by difference Fourier maps and least-squares cycles utilizing SHELXL-97.[2] All calculations were performed using SHELXL-97 crystallographic software package.[2] Relevant crystallographic data, selected bond distances and angles, atomic coordinates and equivalent isotropic displacement parameters for $RbMgCO_3F$ are given in Tables S1 – S3.

Powder X-ray diffraction

Powder X-ray diffraction (PXRD) experiments on $RbMgCO_3F$ were performed using a PANalytical X'Pert PRO diffractometer equipped with Cu Kα radiation. Data were collected in the 2θ range of 5°-90° with a step size of 0.008° and a scan time of 0.3s. No impurities were observed and the experimental and calculated PXRD are in excellent agreement (Figure S1).

Second-Harmonic Generation (SHG)

Powder SHG measurements were performed on a modified Kurtz-nonlinear optical (NLO) system using a pulsed Nd:YAG laser with a wavelength of 1064 nm and 532 nm. A detailed description of the equipment and methodology has been published.[3]As the powder SHG efficiency has been shown to strongly depend on particle size,[4] $RbMgCO_3F$ was ground and sieved into distinct particle size ranges (<20, 20–45, 45–63, 63–75, 75–90, >90 μm). Relevant comparisons with known SHG materials were made by grinding and sieving crystalline α–SiO_2 ,

$LiNbO_3$ and β-BBO into the same particle size ranges. No index matching fluid was used in any of the experiments.

Piezoelectric Measurements

Converse piezoelectric measurements were performed using a Radiant Technologies RT66A piezoelectric test system with a TREK (model 609E-6) high voltage amplifier, Precision Materials Analyzer, Precision High Voltage Interface and MTI 2000 Fotonic Sensor. $RbMgCO_3F$ was pressed into pellets (~1.2 cm diameter, ~ 0.7 mm thickness) and sintered at 330°C for 3 days. Silver paste was applied to both sides of the pellet, and the pellet was cured at 250°C for 12 hours (Figure S2). For all of the structural figures, the program VESTA was used.[5]

Infrared (IR) spectroscopy

The Fourier transform infrared spectroscopy (FTIR) spectrum for $RbMgCO_3F$ was collected on a Bruker Tensor 37 FTIR with the use of a KBr pellet pressed at 15000 PSI. A total of 64 scans were recorded and a background spectrum was subtracted (Figure S3).

UV-Vis diffuse reflectance and transmission spectroscopy

UV-visible diffuse reflectance and transmission data of $RbMgCO_3F$ were collected on a Cary 5000 UV-vis-NIR spectrophotometer over the 200–2000 and 175–2000 nm spectral range, for diffuse reflectance and transmission (Figure S4), respectively, at room temperature.

Thermal analysis

Thermogravimetric analyses were performed on an EXSTAR TG/DTA 6300 instrument. Approximately 20 mg of $RbMgCO_3F$ were placed separately in a platinum pan and heated at a rate of 10°C min^{-1} from room temperature to 900°C under flowing N_2 (Figure S5).

Electronic Structure Calculations

All the density functional theory (DFT) calculations were carried out using Vienna ab initio Simulation Package (VASP)[6-7] within the PBEsol[8] generalized gradient approximation with a planewave cutoff of 540 eV. The electron and ion interaction was described within the projector augmented wave (PAW) method.[9-10] The k-space sampling and integration were done by adopting a 6×6×14 Gamma-centred k-mesh and using the linear tetrahedron method with Blöchl correction,[11] respectively.

Figure S1. Experimental and calculated powder X-ray diffraction patterns of $RbMgCO_3F$

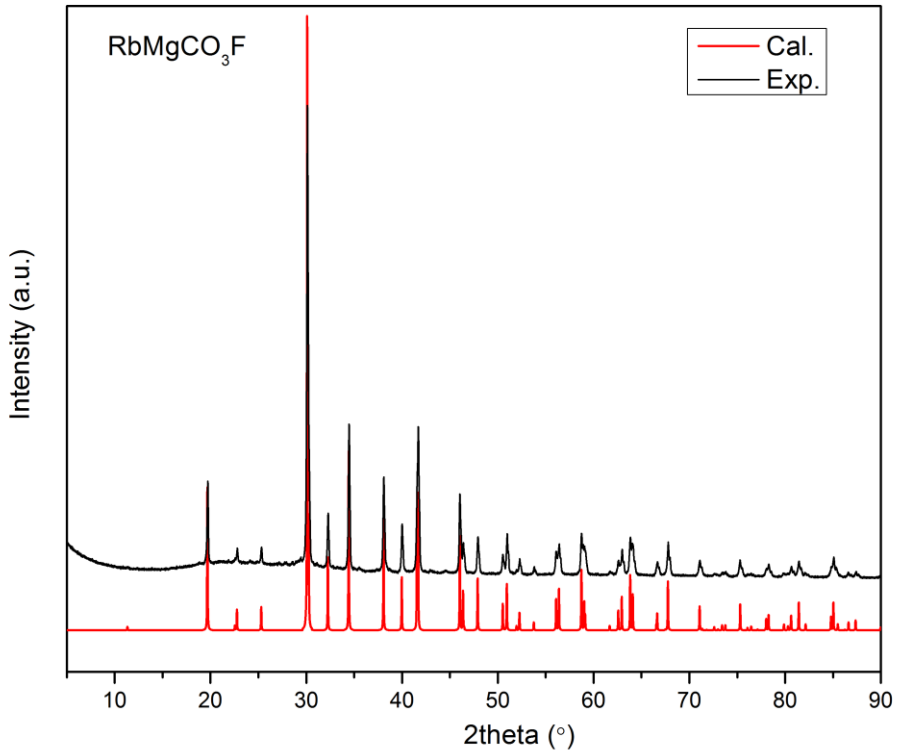

Figure S2. Displacement vs. electric field loops for $RbMgCO_3F$

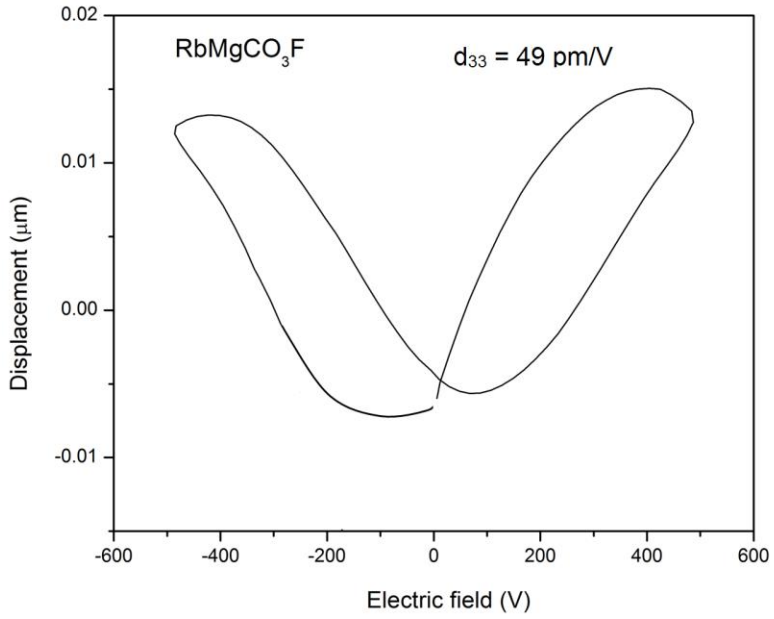

Figure S3. IR spectrum of $RbMgCO_3F$

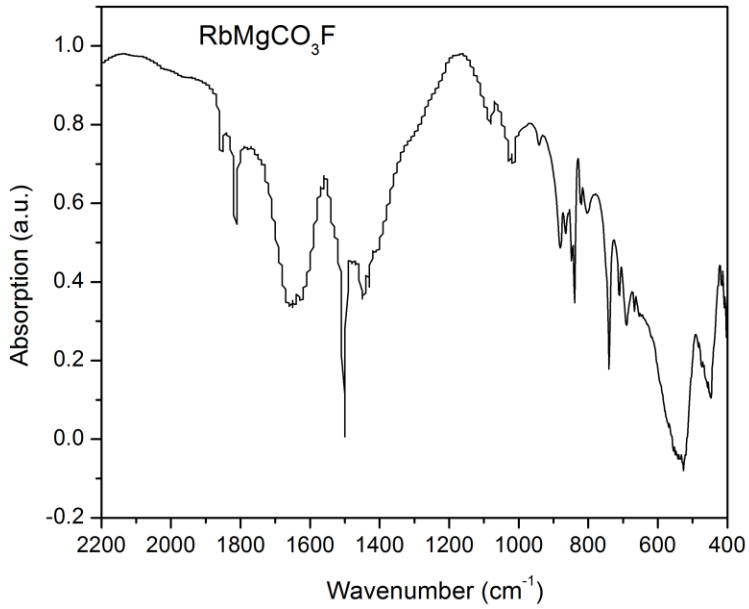

$RbMgCO_3F$	ν(C–O)	δ(OCO)	ν(Mg–O)	ν(Mg–F)
cm^{-1}	1650, 1495	890, 680	830, 790	540, 450

Figure S4. UV-Vis transmission spectrum of $RbMgCO_3F$. Note that the transmission is nearly 50% at 190nm. The 'spike' at ~ 800nm is an artifact attributable to the detector change.

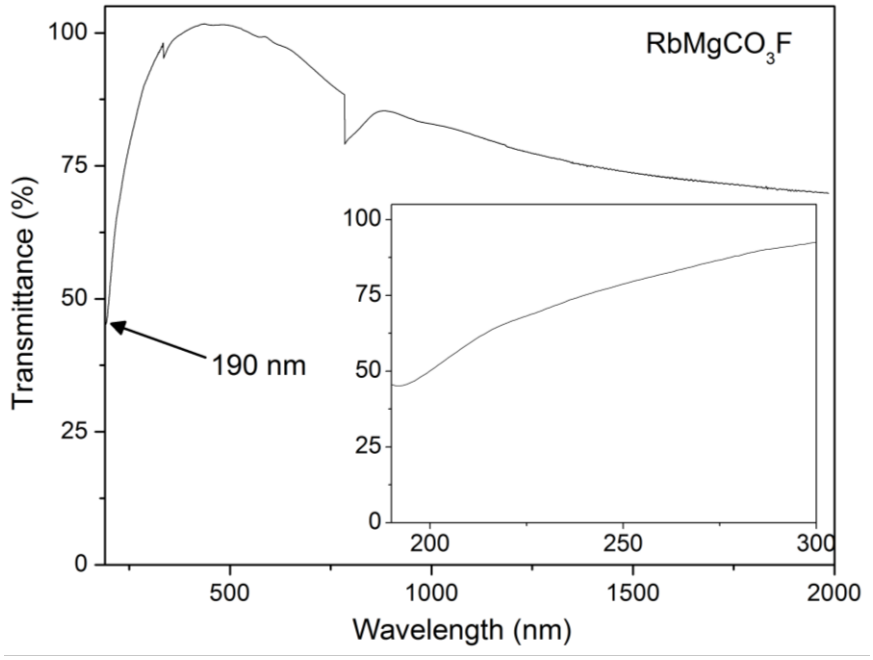

Figure S5. Thermogravimetric analysis and differential thermal analysis diagram of $RbMgCO_3F$ under N_2

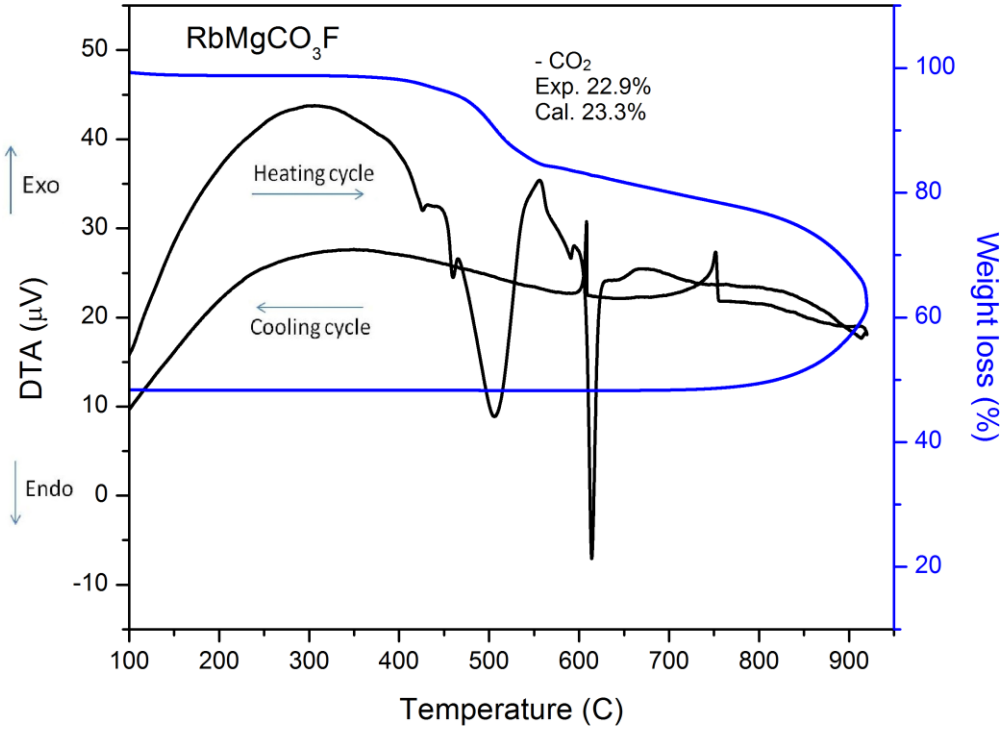

Figure S6. Powder X-ray diffraction of final residuals after TGA/DTA analysis

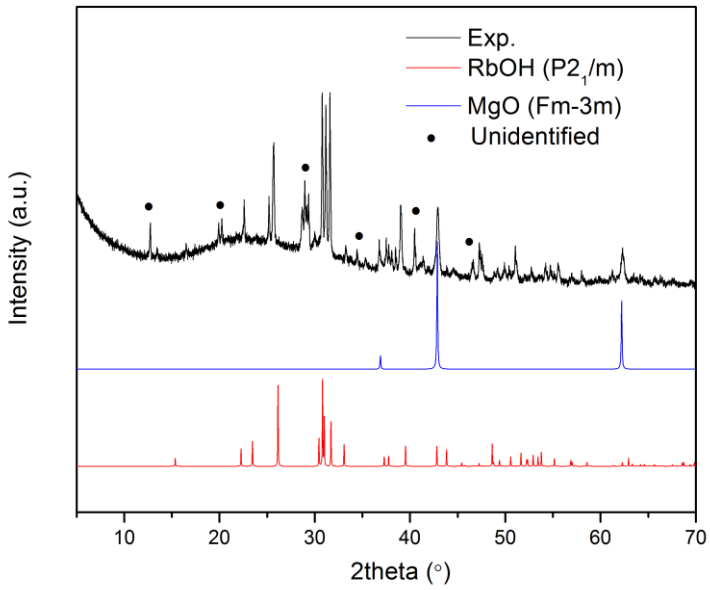

Figure S7. ORTEP representation (50% probability ellipsoids) of $RbMgCO_3F$

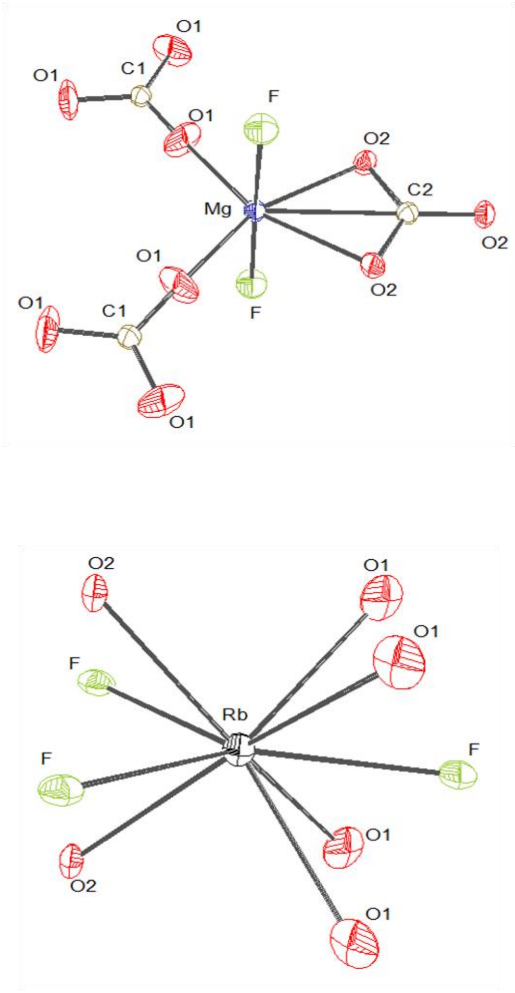

Table S1: Crystallographic data

	$RbMgCO_3F$
$M/gmol^{-1}$	188.79
T/K	293(2)
λ/ Å	0.71073
Crystal system	Hexagonal
Space group	$P\bar{6}2m$ (No. 189)
a/ Å	9.0160(3)
b/ Å	9.0160(3)
c/ Å	3.9403(2)
α/ deg	90
β/ deg	90
γ/ deg	120
$V/ Å^3$	277.39(2)
Z	3
D_c/gcm^{-3}	3.39
μ/mm^{-1}	13.438
$2\theta_{max}/°$	75.52
Number of reflections	572
Number of parameters	28
R_{int}	0.0152
GOF	1.027
$R(F)^a$	0.0087
$R_w(F_o^2)^b$	0.0199
Flack parameter	0.022(5)
Largest diff. peak/hole ($e Å^{-3}$)	0.314/-0.327

[a] $R(F) = \Sigma||F_o| - |F_c||/\Sigma|F_o|$. [b] $R_w(F_o^2) = [\Sigma w(F_o^2 - F_c^2)^2/\Sigma w(F_o^2)^2]^{1/2}$

Table S2. Selected bond distances (Å) and angles (deg)

$RbMgCO_3F$			
Mg – O(1) × 2	1.9937(9)	O(1) – Mg – O(1)	104.03(8)
Mg – O(2) × 2	2.1960(1)	O(1) – Mg – O(2)	97.56(5)
Mg – F × 2	1.9703(2)	O(2) – Mg – O(2)	60.85(6)
C(1) – O(1) × 3	1.2724(11)	F – Mg – O(1)	90.39(2)
C(2) – O(2) × 3	1.2842(7)	F – Mg – O(2)	89.45(3)
		F – Mg – F	178.72(8)

Table S3. Atomic coordinates and equivalent isotropic displacement parameters (Å^2) for $RbMgCO_3F$.

Atom	x	y	z	U_{eq} [a]
Rb	0.0000	0.3825(2)	0.0000	0.0147(4)
Mg	0.0000	0.7188(6)	0.5000	0.0087(9)
C1	0.3333	0.6667	0.5000	0.0094(2)
C2	0.0000	0.0000	0.5000	0.0091(3)
O1	0.2012(2)	0.6833(2)	0.5000	0.0246(2)
O2	0.0000	0.1424(2)	0.5000	0.0117(2)
F	0.2788(2)	0.2788(2)	0.0000	0.0167(2)

[a] U_{eq} is defined as one-third of the trace of the orthogonalized U_{ij} tensor

Table S4. Bond valence analysis for $RbMgCO_3F$[a]

Atom	O1	O2	F	**Σcations**
Rb	0.104 [×4]	0.167 [×2]	0.081 [×2] 0.089	**1.00**
Mg	0.444[×2]	0.257[×2]	0.346 [×2]	**2.09**
C1	1.37 [×3]			**4.11**
C2		1.33 [×3]		**3.99**
Σanions	**1.92**	**1.76**	**0.944**	

[a] Bond valence sums calculated with the formula: $S_i = \exp[(R_0-R_i)/B]$, where S_i=valence of bond "*i*" and B=0.37.

Table S5. Atomic coordinates for $RbMgCO_3F$ in the standard setting for *P*-6*2m* structure (space group no. 189).

Atom	x	y	z	*Wyckoff Site*
Rb	0.3825(2)	0	½	3*f*
Mg	0.7188(6)	0	0	3*g*
C1	⅓	⅔	0	2*d*
C2	0	0	0	1*b*
O1	0.3167(2)	0.5179(2)	0	6*k*
O2	0.1424(2)	0	0	3*g*
F	0.7212(2)	0	½	3*f*

Table S6. Atomic coordinates used in the mode-polarization vector analyses and SAMD calculation[a] for $RbMgCO_3F$ in the ideal *P*-6*2m* structure (space group no. 189). The experimental lattice constants are used for the 'pseudosymmetric' phase. Setting: a=b≠c, α=90°, β=90°, and γ=120°. Atom positions given in reduced units.

Atom	x	y	z	*Wyckoff Site*
Rb	⅓	0	½	3*f*
Mg	⅔	0	0	3*g*
C1	⅓	⅔	0	2*d*
C2	0	0	0	1*b*
O1	⅓	½	0	6*k*
O2	⅙	0	0	3*g*
F	⅔	0	½	3*f*

[a] The specific acentric mode displacements (SAMD) are obtained by computing the square root of the sum of the squared displacements in the convention cell normalized by the unit cell volume ($\Omega = 277.39\text{Å}^3$) as

$$\left[\sum_{\mu,i} m(\mu,i)|\mathbf{u}(\mu,i)|^2\right]^{\frac{1}{2}}/\Omega,$$

where $m(\mu,i)$ is the multiplicity given by the Wyckoff site and $\mathbf{u}(\mu,i)$ is the displacement for atom μ at atomic position i connecting the ideal structure to the noncentrosymmetric structure in units of angstroms. For example: $m(\text{Rb},x)|\mathbf{u}(\text{Rb},x)|^2 = 0.590$ Å^2 whereas $m(\text{Rb},y)|\mathbf{u}(\text{Rb},y)|^2 = m(\text{Rb},z)|\mathbf{u}(\text{Rb},z)|^2 = 0$ Å^2.

References

(1) SAINT; 7.23A ed.; Bruker AXS Inst. Inc.: Madison, WI: 2005.

(2) Sheldrick, G. M. *Acta Crystallogr., Sect. A: Found. Crystallogr.* **2008**, *64*, 112.

(3) Ok, K. M.; Chi, E. O.; Halasyamani, P. S. *Chem. Soc. Rev.* **2006**, *35*, 710.

(4) Kurtz, S. K.; Perry, T. T. *J. Appl. Phys.* **1968**, *39*, 3798.

(5) Momma, K.; Izumi, F. *J. Appl. Crystallogr.* **2011**, *44*, 1272.

(6) Kresse, G.; Hafner, J. *Phys. Rev. B: Condens. Matter* **1993**, *48*, 13115.

(7) Kresse, G.; Furthmüller, J. *Comput. Mater. Sci.* **1996**, *6*, 15.

(8) Perdew, J. P.; Ruzsinszky, A.; Csonka, G. I.; Vydrov, O. A.; Scuseria, G. E.; Constantin, L. A.; Zhou, X.; Burke, K. *Phys. Rev. Lett.* **2008**, *100*, 136406/1.

(9) Blochl, P. E. *Phys. Rev. B: Condens. Matter* **1994**, *50*, 17953.

(10) Kresse, G.; Joubert, D. *Phys. Rev. B: Condens. Matter Mater. Phys.* **1999**, *59*, 1758.

(11) Blochl, P. E.; Jepsen, O.; Andersen, O. K. *Phys. Rev. B: Condens. Matter* **1994**, *49*, 16223.